Entropy **2015**, *17*, 7628-7644; doi:10.3390/e17117628

OPEN ACCESS

entropy

ISSN 1099-4300

www.mdpi.com/journal/entropy

Article

A Memristor-Based Complex Lorenz System and Its Modified Projective Synchronization

Shibing Wang [1,2,*], Xingyuan Wang [1,*] and Yufei Zhou [3]

[1] Faculty of Electronic Information and Electrical Engineering, Dalian University of Technology, Dalian 116024, China

[2] School of Computer and Information Engineering, Fuyang Normal University, Fuyang 236041, China

[3] College of Electrical Engineering and Automation, Anhui University, Hefei 230601, China; E-Mail: zhouyf@ahu.edu.cn

* Authors to whom correspondence should be addressed; E-Mails: wang_shibing@dlut.edu.cn (S.W.); wangxy@dlut.edu.cn (X.W.).

Academic Editors: J.A. Tenreiro Machado and António M. Lopes

Received: 23 September 2015 / Accepted: 29 October 2015 / Published: 5 November 2015

Abstract: The aim of this paper is to introduce and investigate a novel complex Lorenz system with a flux-controlled memristor, and to realize its synchronization. The system has an infinite number of stable and unstable equilibrium points, and can generate abundant dynamical behaviors with different parameters and initial conditions, such as limit cycle, torus, chaos, transient phenomena, *etc.*, which are explored by means of time-domain waveforms, phase portraits, bifurcation diagrams, and Lyapunov exponents. Furthermore, an active controller is designed to achieve modified projective synchronization (MPS) of this system based on Lyapunov stability theory. The corresponding numerical simulations agree well with the theoretical analysis, and demonstrate that the response system is asymptotically synchronized with the drive system within a short time.

Keywords: memristor-based; complex Lorenz system; nonlinear dynamics; modified projective synchronization

PACS Codes: 0545-a; 0545Jn; 0545Pq; 0545Xt

1. Introduction

Memristor is a passive two-terminal fundamental circuit element with the characteristics of nonlinearity, non-volatility, low power consumption, *etc.* It has widely potential applications in electronic circuits and systems, neural networks, computer memory, nonlinear science, and so on. In recent years, generation and nonlinear analyses of memristor-based chaotic systems have attracted more and more attention, and become a research hotspot. By replacing Chua's diodes with memristors, adding memristors to existing nonlinear systems, and designing new systems with memristors, some new chaotic and hyperchaotic systems have been constructed, such as a memristor-based Chua's circuit [1–6], memristor-based van der Pol oscillator [7], memristor-based Lorenz system [8–10], memristor-based Chen system [11], memristor-based Lü system [12], *etc*. Theoretical analyses, numerical simulations and circuit experiments consistently indicate that such memristor-based systems can exhibit complex dynamical behaviours including various bifurcation [1–12], chaos [1–12], hyperchaos [12–14], coexistence of attractors [15], transient dynamical behaviors [16], and initial state dependent dynamical behaviors [17]. Moreover, several fractional-order memristor-based systems and their dynamical behaviors are presented in [9,18,19]. However, the above-mentioned systems are all real systems, and to our best knowledge, there are no reports of memristor-based complex systems. Complex systems are usually constructed to describe and simulate the physics of detuned lasers, rotating fluids, disk dynamos, electronic circuits, *etc.* Several chaotic and hyperchaotic complex systems have been proposed in [20–22]. The studies have revealed more abundant dynamical behaviors of such complex systems, and have concluded that chaotic secure communication with complex systems can increase transmission contents, and enhance anti-attack ability. Due to the advantages of memristor and complex system, it is meaningful and challenging for researchers to construct memristor-based complex systems and to investigate their synchronization for secure communication.

Chaos synchronization plays an important role in secure communication, digital cryptography, image encryption, signal and control processing, *etc.* [22–29], and it has been a popular research area. Recently, a number of control schemes have been developed to achieve various synchronization of memristor-based systems and complex systems. The adopted synchronization schemes include adaptive control [30–32], backstepping control [33], fuzzy control [8], impulsive control [34,35], *etc.* The realized synchronization types include complete synchronization [36,37], anti-synchronization [32], projective synchronization [23,38], lag synchronization [24,39], combination synchronization [40,41], compound synchronization [10], *etc*. However, to our best knowledge, memristor-based complex systems are not involved in the existing literature, unfortunately.

Motivated by the above discussions, this paper aims to construct a novel complex Lorenz system with a flux-controlled memristor, and to realize modified projective synchronization (MPS) of two identical memristor-based complex Lorenz systems. The system is generated from a 4D (four-dimensional) memristor-based real Lorenz system by replacing two real variables to complex variables, which can be expressed as a 6D (six-dimensional) real ordinary differential equations (ODEs). Symmetry and invariance, dissipation, equilibria and stability of the system are analyzed theoretically. Dynamical behaviors are numerically investigated by means of bifurcation diagram, Lyapunov exponent, time-domain waveform, and phase portrait. Fixed points, limit cycles, torus, chaos, and transient behaviors are revealed in the system with different parameters and initial conditions. Furthermore, MPS

is designed to synchronize the memristor-based Lorenz systems quickly and efficiently, which is verified by numerical simulations.

The rest of this paper is organized as follows. In Section 2, a novel memristor-based complex Lorenz system is proposed, and its properties are analyzed theoretically. In Section 3, dynamical behaviors of the system are explored numerically. In Section 4, an active controller is designed to realize MPS for identical memristor-based complex Lorenz systems, and numerical simulations are presented to illustrate the effectiveness of the proposed scheme. Finally, some conclusions are drawn in Section 5.

2. A Novel Memristor-Based Complex Lorenz System and Its Properties

In this section, we construct a novel memristor-based complex Lorenz system and analyze its properties including symmetry, dissipation, equilibria and stability.

2.1. Memristor Model

Memristor, a nonlinear resistor with memory effect, is defined by $f(\varphi, q) = 0$, which includes flux-controlled memristor and charge-controlled memristor. Equations (1) and (2) describe flux-controlled memristor and charge-controlled memristor respectively [42]:

$$W(\varphi) = \frac{dq(\varphi)}{d\varphi}, \ i(t) = W(\varphi)v(t), \ v = \frac{d\varphi(t)}{dt} \tag{1}$$

$$M(q) = \frac{d\varphi(q)}{dq}, \ v(t) = M(q)i(t), \ i = \frac{dq(t)}{dt} \tag{2}$$

where φ and q denote magnetic flux and charge; i and v denote the device terminal current and voltage; $W(\varphi)$ and $M(q)$ denote memductance and memristance which are characterized by a piece-wise linear function [1], smooth continuous cubic nonlinear function [13], Chebyshev polynomials [19], *etc.* In this paper, a flux-controlled memristor with cubic nonlinear characteristics is considered to be:

$$q(\varphi) = \alpha\varphi + \beta\varphi^3, \ W(\varphi) = \frac{dq(\varphi)}{d\varphi} = \alpha + 3\beta\varphi^2 \tag{3}$$

where α and β are positive parameters.

2.2. Memristor-Based Complex Lorenz System

In [8], a modified Lorenz system with a flux-controlled memristor is described by:

$$\begin{cases} \dot{x}_1 = -a_1 x_1 - W(x_4)x_1 + a_2 x_2 \\ \dot{x}_2 = a_3 x_1 - x_2 - x_1 x_3 \\ \dot{x}_3 = x_1 x_2 - a_4 x_3 \\ \dot{x}_4 = -x_1 \end{cases} \tag{4}$$

where a_1, a_2, a_3, a_4 are positive parameters, $W(x_4)$ is memductance characterized by $W(x_4) = \alpha + 3\beta x_4^2$ in this paper. By replacing real variables x_1, x_2 with complex variables, we construct a memristor-based complex Lorenz system of the form:

$$\begin{cases} \dot{x}_1 = -(a_1+\alpha)x_1 + a_2 x_2 - 3\beta x_1 x_4^2 \\ \dot{x}_2 = a_3 x_1 - x_2 - x_1 x_3 \\ \dot{x}_3 = (1/2)(x_1\overline{x}_2 + \overline{x}_1 x_2) - a_4 x_3 \\ \dot{x}_4 = -(1/2)(\overline{x}_1 + x_1) \end{cases} \tag{5}$$

where a_1, a_2, a_3, a_4, α, β are positive parameters, x_1, x_2 are complex variables, x_3, x_4 are real variables, $\overline{x}_1, \overline{x}_2$ denote the complex conjugate variables of x_1, x_2 , $\dot{x}_j (j = 1-4)$ denotes derivative with respect to time. If $x_1 = u_1 + iu_2$, $x_2 = u_3 + iu_4$, $x_3 = u_5$, $x_4 = u_6$, $i = \sqrt{-1}$, the system (5) can be rewritten in the form of six real first ODEs:

$$\begin{cases} \dot{u}_1 = -(a_1+\alpha)u_1 + a_2 u_3 - 3\beta u_6^2 u_1 \\ \dot{u}_2 = -(a_1+\alpha)u_2 + a_2 u_4 - 3\beta u_6^2 u_2 \\ \dot{u}_3 = a_3 u_1 - u_3 - u_1 u_5 \\ \dot{u}_4 = a_3 u_2 - u_4 - u_2 u_5 \\ \dot{u}_5 = u_1 u_3 + u_2 u_4 - a_4 u_5 \\ \dot{u}_6 = -u_1 \end{cases} \tag{6}$$

2.3. Properties of the Memristor-Based Complex Lorenz System

2.3.1. Symmetry and Invariance

Due to the invariance of Equation (6) under the transformation from $(u_1, u_2, u_3, u_4, u_5, u_6)$ to $(-u_1, -u_2, -u_3, -u_4, u_5, -u_6)$, the system is symmetrical about the u_5 axes. That is, if $(u_1, u_2, u_3, u_4, u_5, u_6)$ is a solution of system (6), then $(-u_1, -u_2, -u_3, -u_4, u_5, -u_6)$ is also a solution of the system.

2.3.2. Dissipation

The divergence of system (6) is:

$$\begin{aligned} \nabla V &= \sum_{j=1}^{6} \frac{\partial \dot{u}}{\partial u} = -(a_1+\alpha) - 3\beta u_6^2 - (a_1+\alpha) - 3\beta u_6^2 - 1 - 1 - a_4 \\ &= -2(a_1+\alpha+1) - 6\beta u_6^2 - a_4 \end{aligned} \tag{7}$$

where a_1, a_4, α, β are positive parameters as mentioned, which can guarantee $\nabla V < 0$, so the system (6) is dissipative.

2.3.3. Equilibria and Stability

By solving $\dot{u}_1 = \dot{u}_2 = \dot{u}_3 = \dot{u}_4 = \dot{u}_5 = \dot{u}_6 = 0$, we can obtain the equilibria of system (6):

$$\begin{cases} E_{01} = \{(u_1, u_2, u_3, u_4, u_5, u_6) | u_1 = u_2 = u_3 = u_4 = u_5 = 0, u_6 = c\} \\ E_{02} = \{(u_1, u_2, u_3, u_4, u_5, u_6) | u_1 = 0, u_2 = m, u_3 = 0, u_4 = n, u_5 = p, u_6 = c\} \\ E_{03} = \{(u_1, u_2, u_3, u_4, u_5, u_6) | u_1 = 0, u_2 = -m, u_3 = 0, u_4 = -n, u_5 = -p, u_6 = c\} \end{cases} \tag{8}$$

where $m, n, p, c \in \mathrm{R}$, and

$$m = \sqrt{-a_4(a_1+\alpha+3\beta c^2)(a_1+\alpha-a_2a_3+3\beta c^2)}\Big/(a_1+\alpha+3\beta c^2)$$
$$n = \sqrt{-a_4(a_1+\alpha+3\beta c^2)(a_1+\alpha-a_2a_3+3\beta c^2)}\Big/a_2$$
$$p = \sqrt{-(a_1+\alpha-a_2a_3+3\beta c^2)}\Big/a_2$$

The system has infinite equilibrium points, in which, E_{01} represents the equilibrium points on u_6 axes, obviously. For convenient description, we study the stability of E_{01}, and the Jacobian matrix of system (6) at E_{01} is calculated as:

$$J_{E_{01}} = \begin{bmatrix} -(a_1+\alpha+3\beta c^2) & 0 & a_2 & 0 & 0 & 0 \\ 0 & -(a_1+\alpha+3\beta c^2) & 0 & a_2 & 0 & 0 \\ a_3 & 0 & -1 & 0 & 0 & 0 \\ 0 & a_3 & 0 & -1 & 0 & 0 \\ 0 & 0 & 0 & 0 & -a_4 & 0 \\ -1 & 0 & 0 & 0 & 0 & 0 \end{bmatrix} \tag{9}$$

The characteristic polynomial of Equation (9) is:

$$\lambda(\lambda+a_4)[\lambda^2+(a_1+\alpha+3\beta c^2+1)\lambda+(a_1+\alpha+3\beta c^2-a_2a_3)]^2 = 0 \tag{10}$$

The eigenvalues of Equation (10) are:

$$\begin{aligned} \lambda_1 &= 0 \\ \lambda_2 &= -a_4 \\ \lambda_3 = \lambda_4 &= \frac{-(1+a_1+\alpha+3\beta c^2)}{2} - \frac{\sqrt{(1-a_1-\alpha-3\beta c^2)^2+4a_2a_3}}{2} \\ \lambda_5 = \lambda_6 &= \frac{-(1+a_1+\alpha+3\beta c^2)}{2} + \frac{\sqrt{(1-a_1-\alpha-3\beta c^2)^2+4a_2a_3}}{2} \end{aligned} \tag{11}$$

Since a_1, a_2, a_3, a_4, α, β are positive, the system of (6) has a zero eigenvalue (λ_1) and three negative eigenvalues (λ_2, λ_3, λ_4). According to the Routh–Hurwitz theorem, the necessary and sufficient condition for the other roots to have negative real parts is if and only if $a_1+\alpha+3\beta c^2-a_2a_3>0$, *i.e.*, if the inequality constraint is satisfied and the equilibrium points are stable, and vice versa. Therefore, the system has infinite stable and unstable equilibrium points with different parameters.

3. Dynamical Behaviors of the Memristor-Based Complex Lorenz System

In this section, we explore dynamical behaviors of the memristor-based complex Lorenz system with different parameters and initial conditions based on conventional numerical methods.

3.1. Dynamical Behaviors with Different Parameters

In order to reveal dynamical behaviors of the proposed memristor-based complex Lorenz system, we fix $a_1=8$, $a_2=11$, $a_4=8/3$, $\alpha=0.67\times10^{-3}$, $\beta=0.02\times10^{-3}$ [9], $u(0)=(2,0,1,4,0.1,0)$ and vary a_3 in range of $[0,200]$. Based on the Wolf algorithm and local maximum method, Lyapunov exponents and a bifurcation diagram are calculated and plotted with different computational time intervals 0–3000 s and

0–30000 s as shown in Figures 1 and 2, respectively, which can provide an overall perspective view of the system. However, the two figures are not consistent to each other, apparently, and Figure 2 is different from Figure 1 in some intervals of a_3, e.g., $(18.2, 45.3]$, $[87.6, 92.2]$, $[161.4, 200]$, which indicates that transient dynamical behaviors exist in such intervals due to a boundary crisis [16]. For the sake of exploring the dynamical behaviors in detail, time-domain waveforms, phase portraits, and Lyapunov exponents against time are presented under some fixed parameters as shown in Figures 3–8.

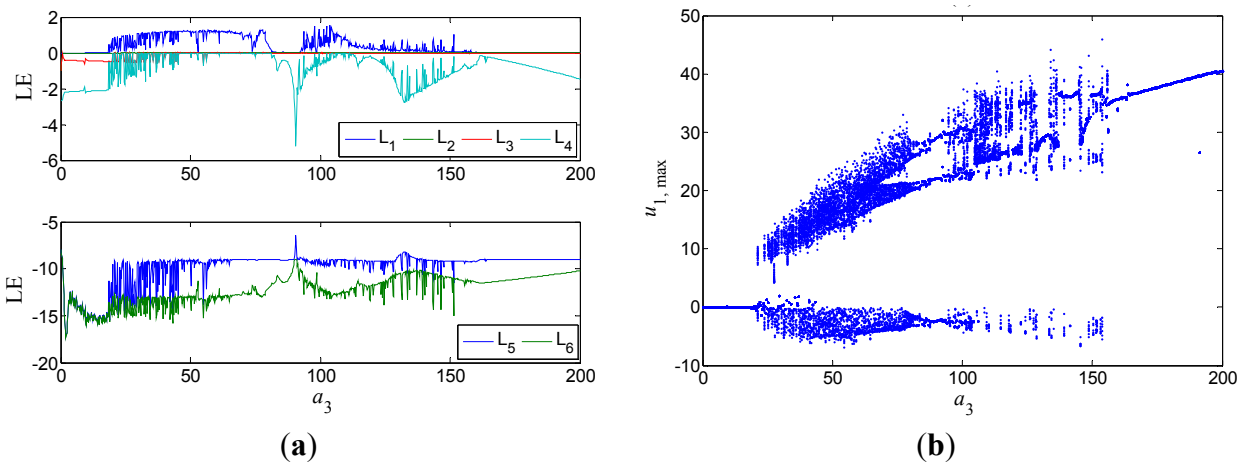

Figure 1. Dynamical behaviors with computational time interval 0–3000 s. (**a**) Lyapunov exponents; (**b**) bifurcation diagram.

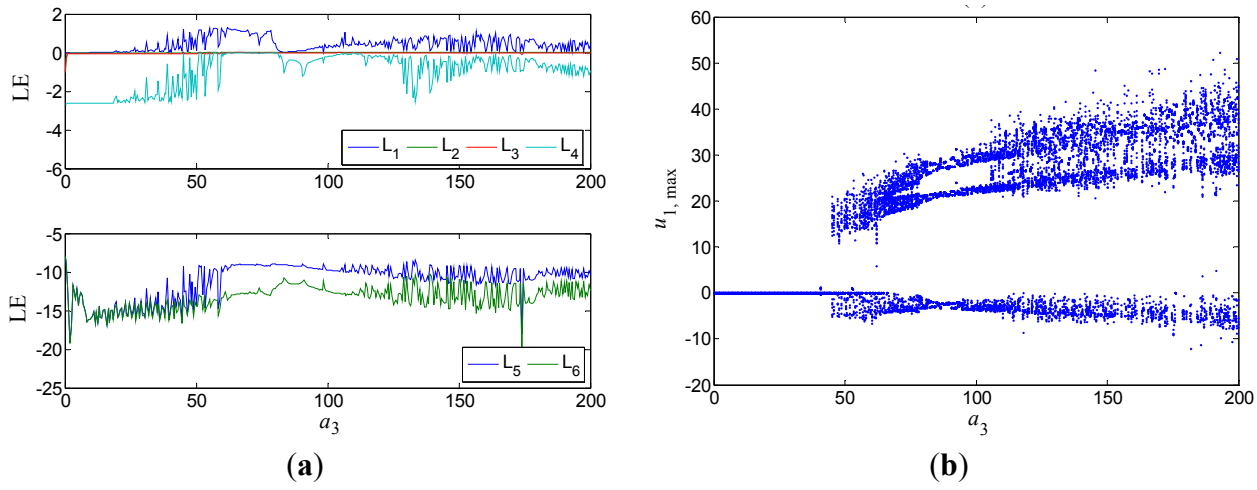

Figure 2. Dynamical behaviors with computational time interval 0–30000 s. (**a**) Lyapunov exponents; (**b**) bifurcation diagram.

(1) Fixed points exist for $a_3 \in [0, 18.2]$. When $a_3 = 5$, the system converges to a fixed point $E(0,0,0,0,0,-891.2)$, and the six Lyapunov exponents are non-positive as shown in Figure 3.

(2) Transient chaos to fixed points exist for $a_3 \in (18.2, 45.3]$. When $a_3 = 25$, the system goes through transient chaos and converges to fixed point $E(0,0,0,0,0,-2120)$ as shown in Figure 4. One Lyapunov exponent (*i.e.*, L1) is positive incipiently, and then tends to zero asymptotically.

(3) A chaotic zone covers most region of $a_3 \in (45.3, 161.4)$. When $a_3 = 50$, the system operates chaotically with a positive Lyapunov exponent as shown in Figure 5.

(4) Transient chaos to Period-5 orbits exist in a narrow interval $a_3 \in (52.7479,\ 52.7482)$. When $a_3 = 52.7481$, the system goes through transient chaos and Period-5 orbit intermittently, and enters into the steady state of Period-5 eventually, as shown in Figure 6.

(5) Transient Period-3 to tours exist for $a_3 \in [87.6,\ 92.2]$. When $a_3 = 90$, the system operates in Period-3 orbit at first, and then enters into the state of tours as shown in Figure 7.

(6) Transient Period-1 to chaos exist for $a_3 \in [161.4,\ 200]$. When $a_3 = 165$, as shown in Figure 8, in the beginning the system operates in Period-1 orbit, then enters into the state of tours, and slides into a chaotic state in the end. The Lyapunov exponent L1 changes from zero to a positive number.

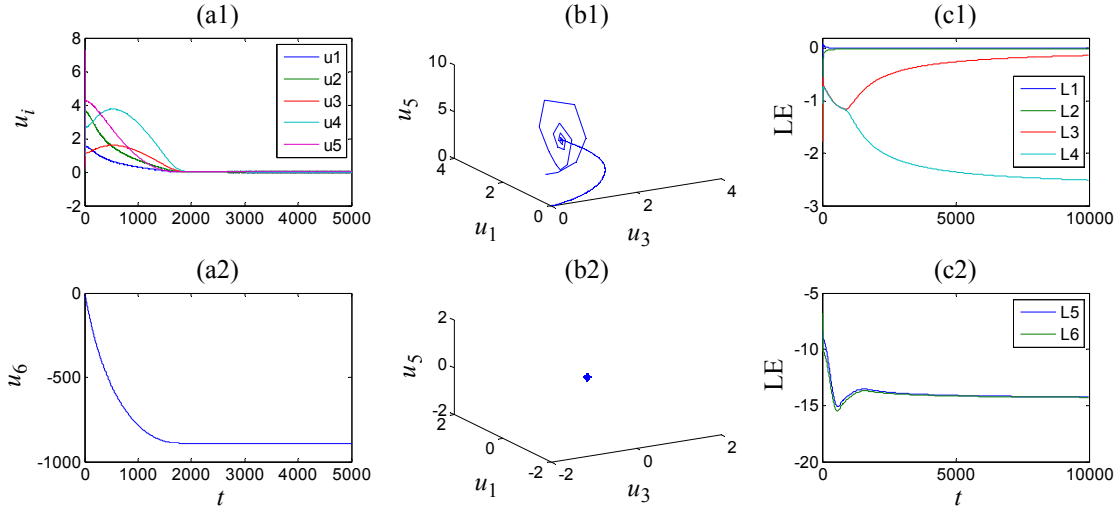

Figure 3. Fixed point ($a_3 = 5$). (**a1**) Waveforms of $u_1 - u_5$; (**a2**) waveform of u_6; (**b1**) phase portrait of transient state; (**b2**) phase portrait of steady state; (**c1**) Lyapunov exponents of $L_1 - L_4$; (**c2**) Lyapunov exponents of $L_5 - L_6$.

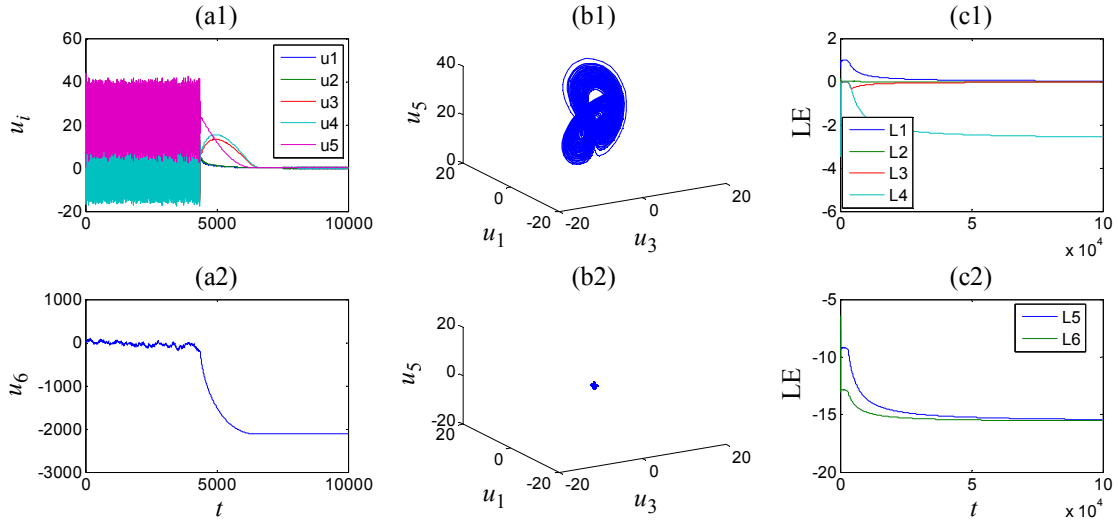

Figure 4. Transient chaos to fixed point ($a_3 = 25$). (**a1**) Waveforms of $u_1 - u_5$; (**a2**) waveform of u_6; (**b1**) phase portrait of transient state; (**b2**) phase portrait of steady state; (**c1**) Lyapunov exponents of $L_1 - L_4$; (**c2**) Lyapunov exponents of $L_5 - L_6$.

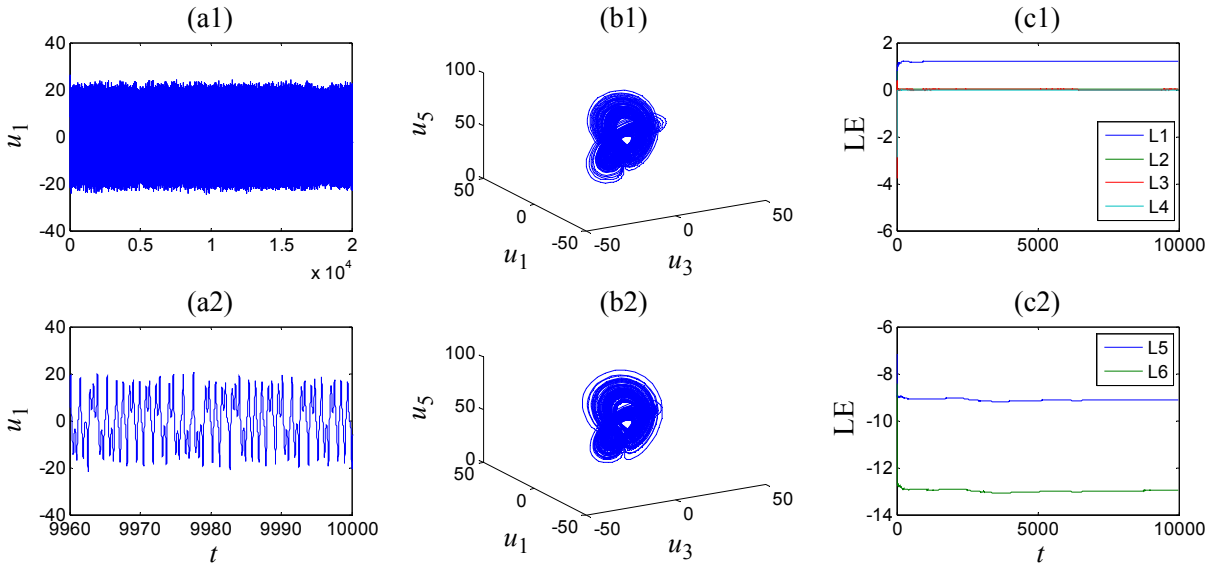

Figure 5. Chaos ($a_3 = 50$). (**a1**) Waveform of u_1 ; (**a2**) subinterval waveform of u_1 ; (**b1**) phase portrait of transient state; (**b2**) phase portrait of steady state; (**c1**) Lyapunov exponents of $L_1 - L_4$; (**c2**) Lyapunov exponents of $L_5 - L_6$.

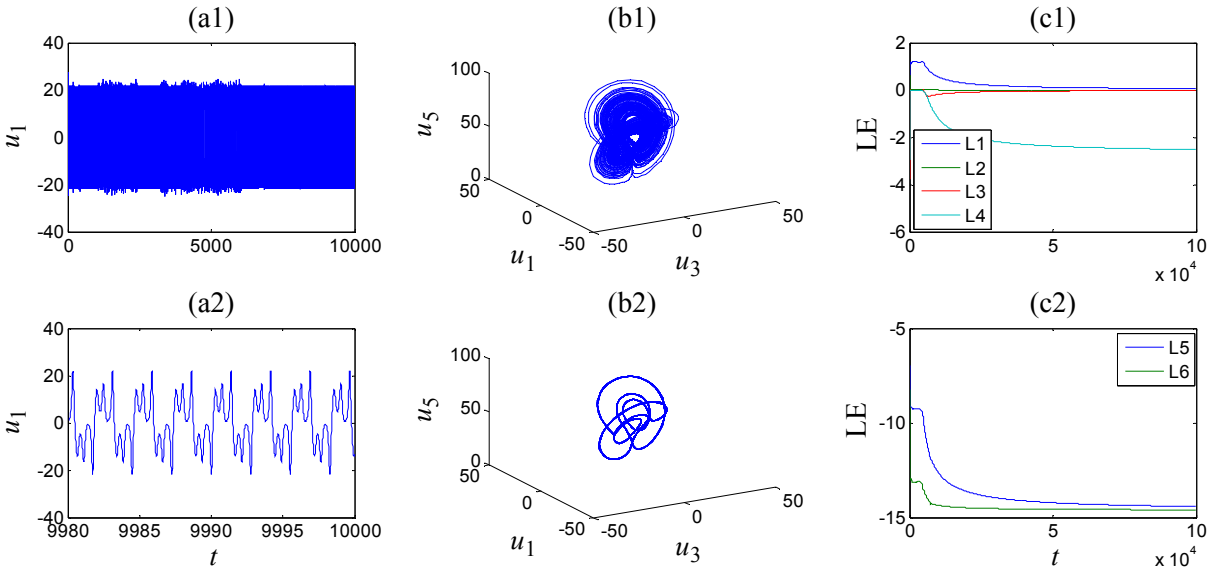

Figure 6. Transient chaos to Period-5 ($a_3 = 52.7481$). (**a1**) Waveform of u_1 ; (**a2**) subinterval waveform of u_1 ; (**b1**) phase portrait of transient state; (**b2**) phase portrait of steady state; (**c1**) Lyapunov exponents of $L_1 - L_4$; (**c2**) Lyapunov exponents of $L_5 - L_6$.

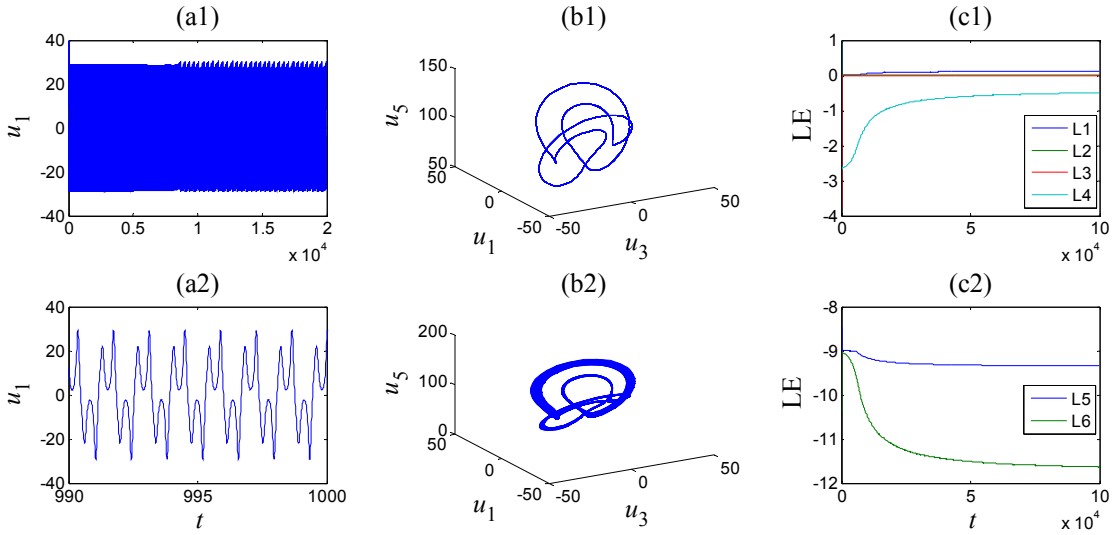

Figure 7. Transient Period-3 to tours ($a_3 = 90$). (**a1**) Waveform of u_1; (**a2**) subinterval waveform of u_1; (**b1**) phase portrait of transient state; (**b2**) phase portrait of steady state; (**c1**) Lyapunov exponents of $L_1 - L_4$; (**c2**) Lyapunov exponents of $L_5 - L_6$.

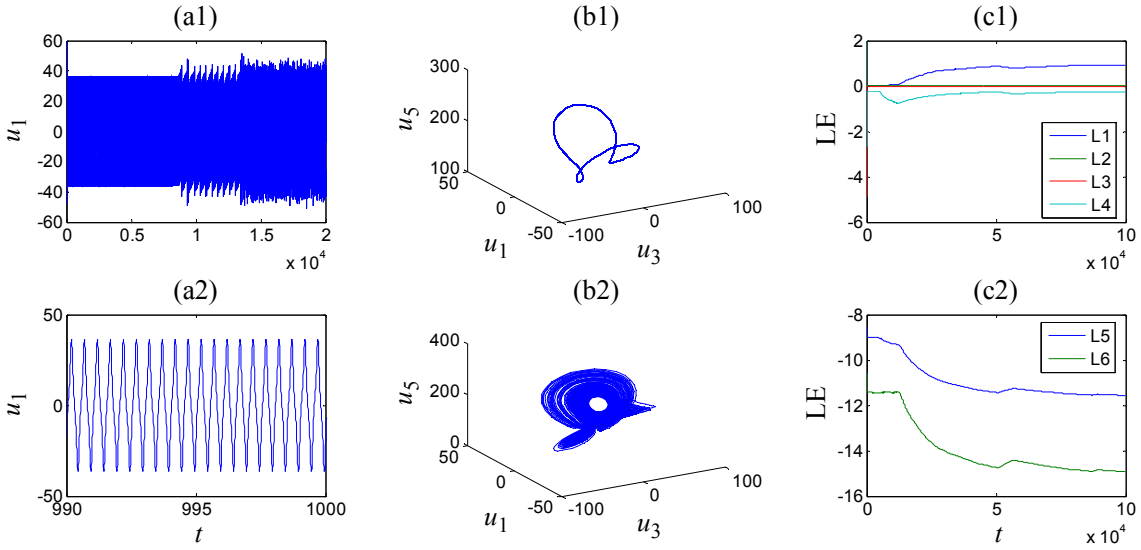

Figure 8. Transient Period-1 to chaos ($a_3 = 165$). (**a1**) Waveform of u_1; (**a2**) subinterval waveform of u_1; (**b1**) phase portrait of transient state; (**b2**) phase portrait of steady state; (**c1**) Lyapunov exponents of $L_1 - L_4$; (**c2**) Lyapunov exponents of $L_5 - L_6$.

Remark 1. Due to transient phenomena, the dynamical behaviors of nonlinear dynamical systems become more complicated and difficult to depict. The time-domain waveform, phase portrait, bifurcation diagram, and Lyapunov exponent should be considered conjunctively, and the computational time interval should be large enough to describe the system behaviors completely and accurately.

3.2. Dynamical Behaviors with Different Initial Conditions

By fixing $a_1 = 8$, $a_2 = 11$, $a_3 = 163$, $a_4 = 8/3$, $\alpha = 0.67 \times 10^{-3}$, $\beta = 0.02 \times 10^{-3}$, $u(0) = (2, 0, 1, 4, 0.1, u_6(0))$, and choosing different $u_6(0)$, we plot time-domain waveforms and phase portraits for system (6) as

shown in Figure 9. The figure indicates that the system operates periodically or chaotically with different initial values of $u_6(0)$; for example, Period-1 limit cycle, Period-1 (red cycle in Figure 9b) to torus, and chaos are found as shown in Figure 9.

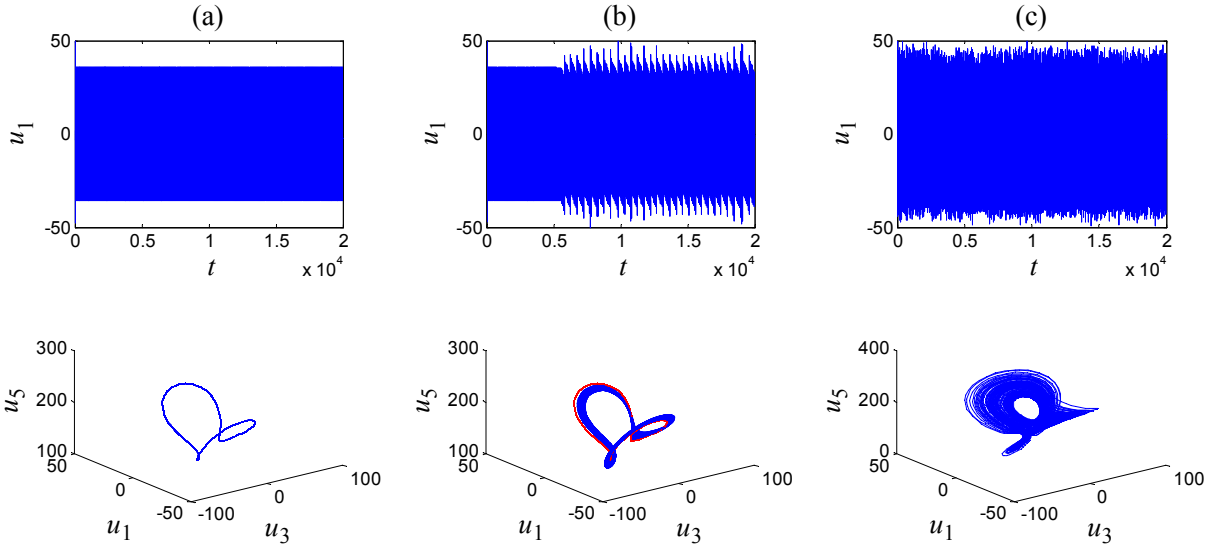

Figure 9. Dynamical behaviors with different initial values of $u_6(0)$. (**a**) Period-1 ($u_6(0)=0$); (**b**) Transient Period-1 to tours ($u_6(0)=3$); (**c**) Chaos ($u_6(0)=300$).

4. MPS of the Memristor-Based Complex Lorenz System

In this section, we study the MPS of two identical memristor-based complex Lorenz systems, and provide numerical simulation results to verify the feasibility and effectiveness of the proposed schemes.

4.1. MPS Design

System (5) is our synchronization object, and the drive system and response system can be described as:

$$\begin{cases} \dot{x}_{1d} = -(a_1+a)x_{1d} + a_2 x_{2d} - 3\beta x_{4d}^2 x_{1d} \\ \dot{x}_{2d} = a_3 x_{1d} - x_{2d} - x_{1d}x_{3d} \\ \dot{x}_{3d} = (1/2)(x_{1d}\overline{x}_{2d} + \overline{x}_{1d}x_{2d}) - a_4 x_{3d} \\ \dot{x}_{4d} = (1/2)(\overline{x}_{1d} + x_{1d}) \end{cases} \tag{12}$$

$$\begin{cases} \dot{x}_{1r} = -(a_1+a)x_{1r} + a_2 x_{2r} - 3\beta x_{4r}^2 x_{1r} + L_1 \\ \dot{x}_{2r} = a_3 x_{1r} - x_{2r} - x_{1r}x_{3r} + L_2 \\ \dot{x}_{3r} = (1/2)(x_{1r}\overline{x}_{2r} + \overline{x}_{1r}x_{2r}) - a_4 x_{3r} + L_3 \\ \dot{x}_{4r} = (1/2)(\overline{x}_{1r} + x_{1r}) + L_4 \end{cases} \tag{13}$$

where $x_{1d} = u_{1d} + iu_{2d}$, $x_{2d} = u_{3d} + iu_{4d}$, $x_{1r} = u_{1r} + iu_{2r}$, $x_{2r} = u_{3r} + iu_{4r}$ are complex state variables, $x_{3d} = u_{5d}$, $x_{4d} = u_{6d}$, $x_{3r} = u_{5r}$, $x_{4r} = u_{6r}$ are real state variables, $L_1 = v_1 + iv_2$, $L_2 = v_3 + iv_4$, $L_3 = v_5$, $L_4 = v_6$ are control functions, and then the complex systems (12) and (13) can be described by real Equation (14) and Equation (15) respectively:

$$\begin{cases} \dot{u}_{1d} = -(a_1+\alpha)u_{1d} + a_2u_{3d} - 3\beta u_{6d}^2 u_{1d} \\ \dot{u}_{2d} = -(a_1+\alpha)u_{2d} + a_2u_{4d} - 3\beta u_{6d}^2 u_{2d} \\ \dot{u}_{3d} = a_3u_{1d} - u_{3d} - u_{1d}u_{5d} \\ \dot{u}_{4d} = a_3u_{2d} - u_{4d} - u_{2d}u_{5d} \\ \dot{u}_{5d} = u_{1d}u_{3d} + u_{2d}u_{4d} - a_4u_{5d} \\ \dot{u}_{6d} = -u_{1d} \end{cases} \tag{14}$$

$$\begin{cases} \dot{u}_{1r} = -(a_1+\alpha)u_{1r} + a_2u_{3r} - 3\beta u_{6r}^2 u_{1r} + v_1 \\ \dot{u}_{2r} = -(a_1+\alpha)u_{2r} + a_2u_{4r} - 3\beta u_{6r}^2 u_{2r} + v_2 \\ \dot{u}_{3r} = a_3u_{1r} - u_{3r} - u_{1r}u_{5r} + v_3 \\ \dot{u}_{4r} = a_3u_{2r} - u_{4r} - u_{2r}u_{5r} + v_4 \\ \dot{u}_{5r} = u_1u_{3r} + u_{2r}u_{4r} - a_4u_{5r} + v_5 \\ \dot{u}_{6r} = -u_{1r} + v_6 \end{cases} \tag{15}$$

Errors between the drive system (12) and the response system (13) are defined as:

$$\begin{cases} e_1 = e_{u1} + ie_{u2} = (u_{1d} - k_1u_{1r}) + i(u_{2d} - k_2u_{2r}) \\ e_2 = e_{u3} + ie_{u4} = (u_{3d} - k_3u_{3r}) + i(u_{4d} - k_4u_{4r}) \\ e_3 = e_{u5} = u_{5d} - k_5u_{5r} \\ e_4 = e_{u6} = u_{6d} - k_6u_{6r} \end{cases} \tag{16}$$

where $e_{u1} = u_{1d} - k_1u_{1r}$, $e_{u2} = u_{2d} - k_2u_{2r}$, $e_{u3} = u_{3d} - k_3u_{3r}$, $e_{u4} = u_{4d} - k_4u_{4r}$, $e_{u5} = u_{5d} - k_5u_{5r}$, $e_{u6} = u_{6d} - k_6u_{6r}$, which are errors between systems (14) and (15), $k_j\,(j = 1-6)$ denotes projective factor. By substituting Equations (14) and (15), we can obtain the derivative of $e_{ui}\,(i = 1-6)$ as:

$$\begin{cases} \dot{e}_{u1} = -(a_1+\alpha)e_{u1} + a_2u_{3d} - 3\beta u_{6d}^2 u_{1d} - k_1(a_2u_{3r} - 3\beta u_{6r}^2 u_{1r}) - k_1v_1 \\ \dot{e}_{u2} = -(a_1+\alpha)e_{u2} + a_2u_{4d} - 3\beta u_{6d}^2 u_{2d} - k_2(a_2u_{4r} - 3\beta u_{6r}^2 u_{2r}) - k_2v_2 \\ \dot{e}_{u3} = -e_{u3} + a_3u_{1d} - u_{1d}u_{5d} - k_3(a_3u_{1r} - u_{1r}u_{5r}) - k_3v_3 \\ \dot{e}_{u4} = -e_{u4} + a_3u_{2d} - u_{2d}u_{5d} - k_4(a_3u_{2r} - u_{2r}u_{5r}) - k_4v_4 \\ \dot{e}_{u5} = -a_4e_{u5} + u_{1d}u_{3d} + u_{2d}u_{4d} - k_5(u_{1r}u_{3r} + u_{2r}u_{4r}) - k_5v_5 \\ \dot{e}_{u6} = -e_{u6} + u_{6d} - u_{1d} - k_6(u_{6r} - u_{1r}) - k_6v_6 \end{cases} \tag{17}$$

Theorem 1. The MPS between the drive system (12) and the response system (13) can be achieved, if the controllers are designed as

$$\begin{cases} v_1 = [a_2u_{3d} - 3\beta u_{6d}^2 u_{1d} - k_1(a_2u_{3r} - 3\beta u_{6r}^2 u_{1r})]/k_1 \\ v_2 = [a_2u_{4d} - 3\beta u_{6d}^2 u_{2d} - k_2(a_2u_{4r} - 3\beta u_{6r}^2 u_{2r})]/k_2 \\ v_3 = [a_3u_{1d} - u_{1d}u_{5d} - k_3(a_3u_{1r} - u_{1r}u_{5r})]/k_3 \\ v_4 = [a_3u_{2d} - u_{2d}u_{5d} - k_4(a_3u_{2r} - u_{2r}u_{5r})]/k_4 \\ v_5 = [u_{1d}u_{3d} + u_{2d}u_{4d} - k_5(u_{1r}u_{3r} + u_{2r}u_{4r})]/k_5 \\ v_6 = [u_{6d} - u_{1d} - k_6(u_{6r} - u_{1r})]/k_6 \end{cases} \tag{18}$$

Proof. Choose the Lyapunov function as:

$$V(t) = \frac{1}{2}\sum_{j=1}^{6} e_{uj}^2 = \frac{1}{2}(e_{u1}^2 + e_{u2}^2 + e_{u3}^2 + e_{u4}^2 + e_{u5}^2 + e_{u6}^2) \tag{19}$$

Solve the derivative of $V(t)$ along the trajectory of error system (16):

$$\begin{aligned}
\dot{V}(t) &= \sum_{i=1}^{6} e_{uj}\dot{e}_{uj} \\
&= e_{u1}[-(a_1+\alpha)e_{u1} + a_2u_{3d} - 3\beta u_{6d}^2 u_{1d} - k_1(a_2u_{3r} - 3\beta u_{6r}^2 u_{1r}) - k_1v_1] \\
&+e_{u2}[-(a_1+\alpha)e_{u2} + a_2u_{4d} - 3\beta u_{6d}^2 u_{2d} - k_2(a_2u_{4r} - 3\beta u_{6r}^2 u_{2r}) - k_2v_2] \\
&+e_{u3}[-e_{u3} + a_3u_{1d} - u_{1d}u_{5d} - k_3(a_3u_{1r} - u_{1r}u_{5r}) - k_3v_3] \\
&+e_{u4}[-e_{u4} + a_3u_{2d} - u_{2d}u_{5d} - k_4(a_3u_{2r} - u_{2r}u_{5r}) - k_4v_4] \\
&+e_{u5}[-a_4e_{u5} + u_{1d}u_{3d} + u_{2d}u_{4d} - k_5(u_{1r}u_{3r} + u_{2r}u_{4r}) - k_5v_5] \\
&+e_{u6}[-e_{u6} + u_{6d} - u_{1d} - k_6(u_{6r} - u_{1r}) - k_6v_6]
\end{aligned} \tag{20}$$

Substitute Equation (17) into Equation (20), then

$$\dot{V}(t) = -(a_1+\alpha)e_{u1}^2 - (a_1+\alpha)e_{u2}^2 - e_{u3}^2 - e_{u4}^2 - a_4e_{u5}^2 - e_{u6}^2 < 0 \tag{21}$$

According to the Lyapunov stability theory, since $V(t)$ is a positive function and its derivative $\dot{V}(t)$ is negative, the errors e_{uj} ($j = 1-6$) and e_j ($j = 1-4$) tend to zero as $t \to \infty$. Therefore, the response system (13) is synchronized with the drive system (12) asymptotically. □

4.2. Numerical Simulations

To demonstrate the validity of the above-mentioned MPS scheme, we provide numerical simulation results between two identical memristor-based complex Lorenz systems. The parameters and initial conditions are selected as $a_1 = 8$, $a_2 = 11$, $a_3 = 50$, $a_4 = 8/3$, $\alpha = 0.67 \times 10^{-3}$, $\beta = 0.02 \times 10^{-3}$, $u_d(0) = (2, -3, 3, -2, 3, 2)$, $u_r(0) = (-1, -1, 0, 0, 0, -1)$, which can guarantee the drive system operating chaotically. When the projective factors $k_1 = 1$, $k_2 = -1$, $k_3 = 2$, $k_4 = -2$, $k_5 = 0.5$, $k_6 = -0.5$, the results are illustrated in Figures 10, 11 and 12a, which consistently indicate that MPS is achieved within a short time. In detail, Figure 10 presents time-domain waveforms of the drive system (12) and the response system (13), Figure 11 shows that synchronization errors eventually converge to zero within five seconds, and Figure 12a displays phase portrait of $u_1 - u_3 - u_5$ phase space. Furthermore, we investigate the MPS under different scaling factors. When $k_1 = k_2 = -1$, $k_3 = k_4 = 2$, $k_5 = k_6 = 0.5$, MPS is achieved as shown in Figure 12b. When $k_j = -1.5$ ($j = 1-6$) and $k_j = 0.5$ ($j = 1-6$), projective synchronization (PS) is achieved as shown in Figure 12c,d. When $k_j = -1$ ($j = 1-6$), anti-synchronization (AS) is achieved as shown in Figure 12e. When $k_j = 1$ ($j = 1-6$), complete synchronization (CS) is achieved as shown in Figure 12f.

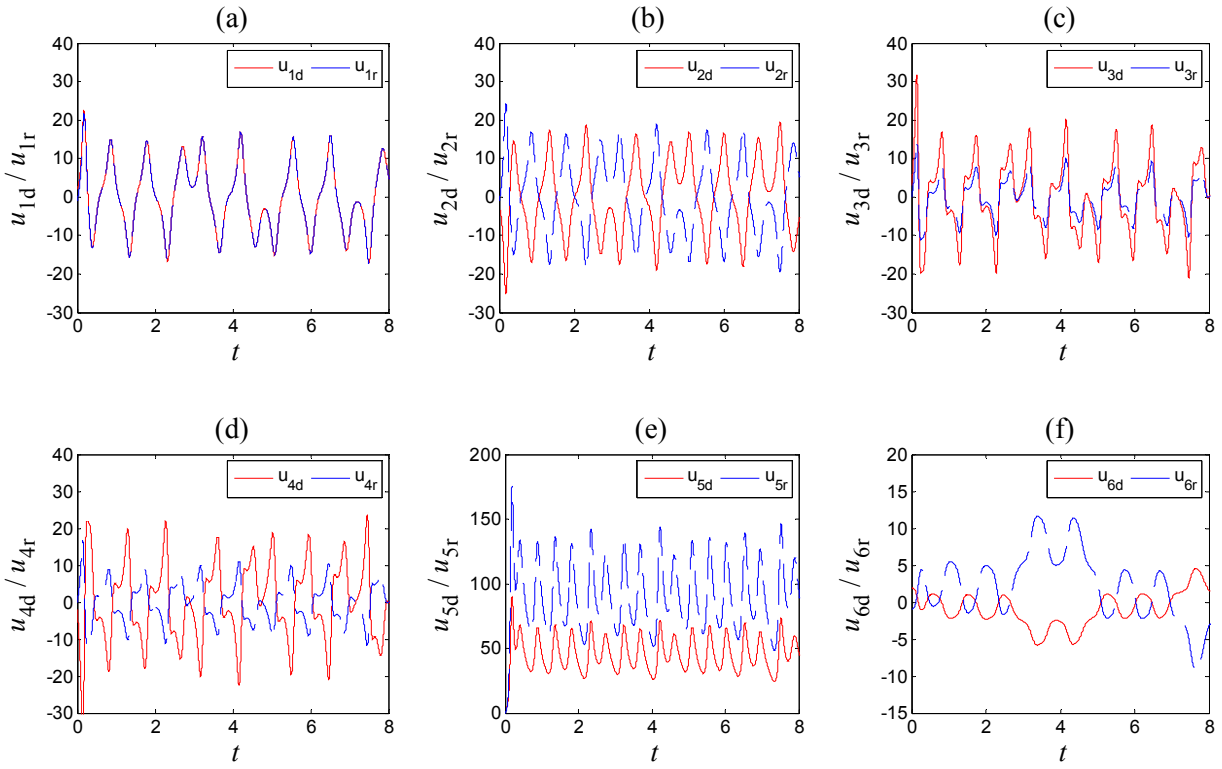

Figure 10. Time-domain waveforms of the drive system (12) and response system (13). **(a)** $u_{1d}=u_{1r}$; **(b)** $u_{2d}=-u_{2r}$; **(c)** $u_{3d}=2u_{3r}$; **(d)** $u_{4d}=-2u_{4r}$; **(e)** $u_{5d}=0.5u_{5r}$; **(f)** $u_{6d}=-0.5u_{6r}$.

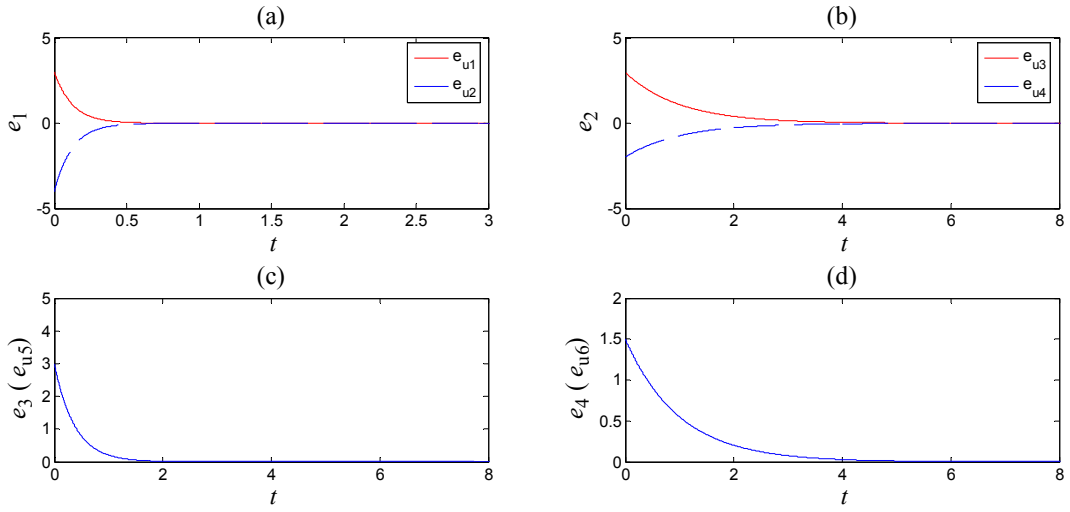

Figure 11. Synchronization errors between the drive system (12) and response system (13). **(a)** $e_1=e_{u1}+ie_{u2}$; **(b)** $e_2=e_{u3}+ie_{u4}$; **(c)** $e_3=e_{u5}$; **(d)** $e_4=e_{u6}$.

Remark 2. It is worth noting that the above MPS of memristor-based complex Lorenz systems can be applied to digital cryptography and secure communication. The sender modulates the original signals into the chaotic sequences generated from memristor-based complex Lorenz system and sends the combined signals to the receiver through communication channels, and the receiver obtains and decodes the combined signals through the MPS. Compared to the conventional synchronization of chaotic real

systems, the complex system can provide multiple state variables to improve the efficiency of information transmission, and MPS can achieve high unpredictability to improve the security of communication.

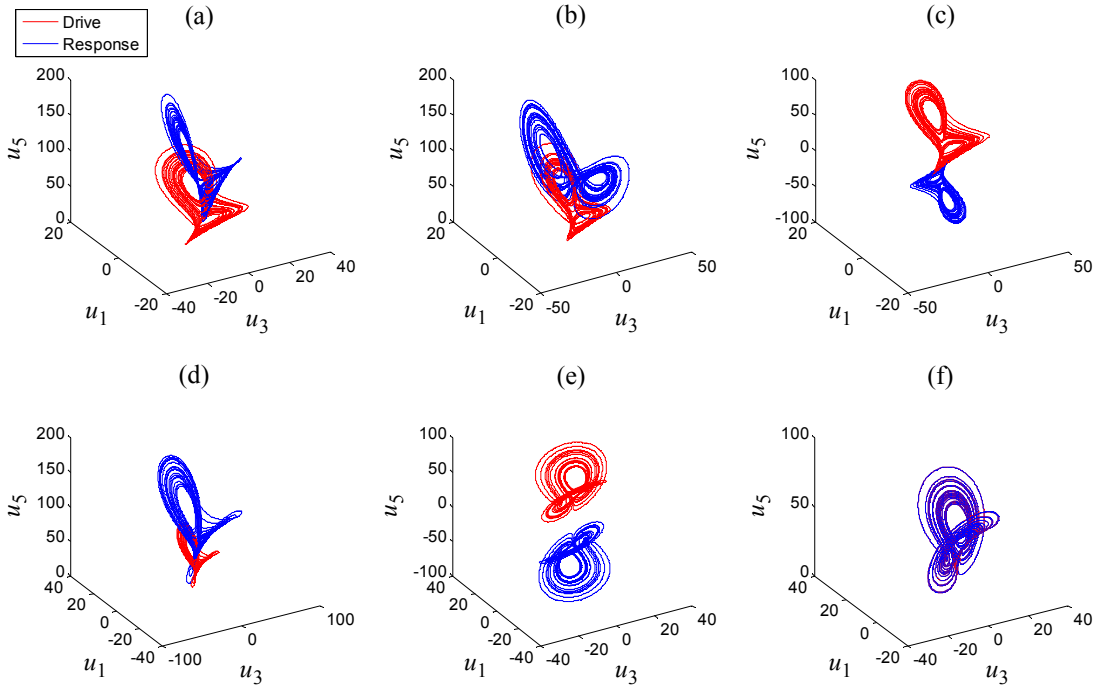

Figure 12. Synchronization with different projective factors. (**a**) $k_1 = 1,\ k_2 = -1,\ k_3 = 2,\ k_4 = -2,\ k_5 = 0.5,\ k_6 = -0.5$; (**b**) $k_1 = k_2 = -1,\ k_3 = k_4 = 2,\ k_5 = k_6 = 0.5$; (**c**) $k_j = -1.5$ $(j = 1-6)$; (**d**) $k_j = 0.5$ $(j = 1-6)$; (**e**) $k_j = -1$ $(j = 1-6)$;(**f**) $k_j = 1$ $(j = 1-6)$.

5. Conclusions

In this paper, a novel complex Lorenz system with a flux-controlled memristor has been constructed and investigated. We found that the proposed system has infinite stable and unstable equilibrium points and exhibits abundant dynamical behaviors including fixed points, limit cycles, tori, chaos, and complex transient behaviors. Furthermore, MPS controller has been designed to synchronize the memristor-based Lorenz systems up to different scaling factors quickly and efficiently, which has been demonstrated by numerical simulations. However, the relevant research has just begun, and the memristor-based complex systems and their synchronization will have to be investigated from the viewpoint of applications in the future.

Acknowledgments

This work was supported by the Natural Science Foundation of China under Grant No. 61370145, No. 61173183, and No. 61071023, Program for Liaoning Excellent Talents in University No. LR2012003, the Natural Science Foundation of Anhui Provincial Universities under Grant No. KJ2012A214 and No. KJ2013B192.

Author Contributions

Xingyuan Wang, Yufei Zhou and Shibing Wang collectively realized theoretical analyses; Shibing Wang performed numerical simulations and wrote the paper. All authors have read and approved the final manuscript.

Conflicts of Interest

The authors declare no conflict of interest.

References

1. Itoh, M.; Chua, L.O. Memristor Oscillators. *Int. J. Bifurc. Chaos* **2008**, *18*, 3183–3206.
2. Muthuswamy, B.; Kokate, P.P. Memristor-based chaotic circuits. *IETE Tech. Rev*. **2009**, *26*, doi:10.4103/0256-4602.57827.
3. Messias, M.; Nespoli, C.; Botta, V.A. Hopf bifurcation from lines of equilibria without parameters in memristor oscillators. *Int. J. Bifurc. Chaos* **2010**, *20*, 437–450.
4. Li, Y.; Huang, X.; Guo, M. The generation, analysis, and circuit implementation of a new memristor based chaotic system. *Math. Probl. Eng.* **2013**, *2013*, doi:10.1155/2013/398306.
5. Ishaq Ahamed, A.; Lakshmanan, M. Nonsmooth bifurcations, transient hyperchaos and hyperchaotic beats in a memristive Murali–Lakshmanan–Chua circuit. *Int. J. Bifurc. Chaos* **2013**, *23*, doi:10.1142/S0218127413500983.
6. Wang, X.; Wang, G.; Wang, X. Dynamic character analysis of a LDR, memristor-based chaotic system. *J. Circuits Syst. Comput.* **2014**, *23*, doi:10.1142/S0218126614500856.
7. Lu, Y.; Huang, X.; He, S.; Wang, D.; Zhang, B. Memristor Based van der Pol oscillation circuit. *Int. J. Bifurc. Chaos* **2014**, *24*, doi:10.1142/S0218127414501545.
8. Wen, S.; Zeng, Z.; Huang, T.; Chen, Y. Fuzzy modeling and synchronization of different memristor-based chaotic circuits. *Phys. Lett. A* **2013**, *377*, 2016–2021.
9. Xi, H.; Li, Y.; Huang, X. Generation and nonlinear dynamical analyses of fractional-order memristor-based Lorenz systems. *Entropy* **2014**, *16*, 6240–6253.
10. Zhang, B.; Deng, F. Double-compound synchronization of six memristor-based Lorenz systems. *Nonlinear Dyn.* **2014**, *77*, 1519–1530.
11. Hu, X.; Chen, G.; Duan, S.; Feng, G. A memristor-based chaotic system with boundary conditions. In *Memristor Networks*; Adamatzky, A., Chua, L., Eds.; Springer: Berlin/Heidelberg, Germany, 2014; pp. 351–364.
12. Li, Q.; Zeng, H.; Li, J. Hyperchaos in a 4D memristive circuit with infinitely many stable equilibria. *Nonlinear Dyn.* **2015**, *79*, 2295–2308.
13. Fitch, A.L.; Yu, D.; Iu, H.H.C.; Sreeram, V. Hyperchaos in a memristor-based modified canonical Chua's circuit. *Int. J. Bifurc. Chaos* **2012**, *22*, doi:10.1142/S0218127412501337.
14. Ma, J.; Chen, Z.; Wang, Z.; Zhang, Q. A four-wing hyper-chaotic attractor generated from a 4-D memristive system with a line equilibrium. *Nonlinear Dyn.* **2015**, *81*, 1275–1288.
15. Chen, M.; Li, M.; Yu, Q.; Bao, B.; Xu, Q.; Wang, J. Dynamics of self-excited attractors and hidden attractors in generalized memristor-based Chua's circuit. *Nonlinear Dyn.* **2015**, *81*, 215–226.

16. Bao, B.; Jiang, P.; Wu, H.; Hu, F. Complex transient dynamics in periodically forced memristive Chua's circuit. *Nonlinear Dyn.* **2015**, *79*, 2333–2343.
17. Bao, B.-C.; Xu, J.-P.; Liu, Z. Initial state dependent dynamical behaviors in a memristor based chaotic circuit. *Chin. Phys. Lett.* **2010**, *27*, doi:10.1088/0256-307X/27/7/070504.
18. Cafagna, D.; Grassi, G. On the simplest fractional-order memristor-based chaotic system. *Nonlinear Dyn.* **2012**, *70*, 1185–1197.
19. Teng, L.; Iu, H.H.C.; Wang, X.; Wang, X. Chaotic behavior in fractional-order memristor-based simplest chaotic circuit using fourth degree polynomial. *Nonlinear Dyn.* **2014**, *77*, 231–241.
20. Fowler, A.C.; Gibbon, J.D.; McGuinness, M.J. The complex Lorenz equations. *Physica D Nonlinear Phenom.* **1982**, *4*, 139–163.
21. Liu, J.; Liu, S.; Zhang, F. A novel four-wing hyperchaotic complex system and its complex modified hybrid projective synchronization with different dimensions. *Abstr. Appl. Anal.* **2014**, *2014*, doi:10.1155/2014/257327.
22. Luo, C.; Wang, X. Chaos generated from the fractional-order complex Chen system and its application to digital secure communication. *Int. J. Mod. Phys. C* **2013**, *24*, doi:10.1142/S0129183113500253.
23. Muthukumar, P.; Balasubramaniam, P.; Ratnavelu, K. Fast projective synchronization of fractional order chaotic and reverse chaotic systems with its application to an affine cipher using date of birth (DOB). *Nonlinear Dyn.* **2015**, *80*, 1883–1897.
24. Zhang, F. Lag synchronization of complex Lorenz system with applications to communication. *Entropy* **2015**, *17*, 4974–4985.
25. Sun, J.; Shen, Y.; Yin, Q.; Xu, C. Compound synchronization of four memristor chaotic oscillator systems and secure communication. *Chaos Interdiscip. J. Nonlinear Sci.* **2013**, *23*, 13140.
26. Balasubramaniam, P.; Muthukumar, P.; Ratnavelu, K. Theoretical and practical applications of fuzzy fractional integral sliding mode control for fractional-order dynamical system. *Nonlinear Dyn.* **2015**, *80*, 249–267.
27. Muthukumar, P.; Balasubramaniam, P.; Ratnavelu, K. Synchronization and an application of a novel fractional order King Cobra chaotic system. *Chaos Interdiscip. J. Nonlinear Sci.* **2014**, *24*, 033105.
28. Muthukumar, P.; Balasubramaniam, P.; Ratnavelu, K. Synchronization of a novel fractional order stretch-twist-fold (STF) flow chaotic system and its application to a new authenticated encryption scheme (AES). *Nonlinear Dyn.* **2014**, *77*, 1547–1559.
29. Muthukumar, P.; Balasubramaniam, P. Feedback synchronization of the fractional order reverse butterfly-shaped chaotic system and its application to digital cryptography. *Nonlinear Dyn.* **2013**, *74*, 1169–1181.
30. Wang, B.; Jian, J.; Yu, H. Adaptive synchronization of fractional-order memristor-based Chua's system. *Syst. Sci. Control Eng.* **2014**, *2*, 291–296.
31. Wen, S.; Zeng, Z.; Huang, T. Adaptive synchronization of memristor-based Chua's circuits. *Phys. Lett. A* **2012**, *376*, 2775–2780.
32. Zhou, X.; Xiong, L.; Cai, W.; Cai, X. Adaptive synchronization and antisynchronization of a hyperchaotic complex Chen system with unknown parameters based on passive control. *J. Appl. Math.* **2013**, *2013*, doi:10.1155/2013/845253.

33. Rakkiyappan, R.; Sivasamy, R.; Li, X. Synchronization of identical and nonidentical memristor-based chaotic systems via active backstepping control technique. *Circuits Syst. Signal Process.* **2015**, *34*, 763–778.
34. Yang, S.; Li, C.; Huang, T. Impulsive control and synchronization of memristor-Based chaotic circuits. *Int. J. Bifurc. Chaos* **2014**, *24*, 1450162.
35. Aly, S.; Al-Qahtani, A.; Khenous, H.B.; Mahmoud, G.M. Impulsive control and synchronization of complex Lorenz systems. *Abstr. Appl. Anal.* **2014**, *2014*, doi:10.1155/2014/932327.
36. El-Sayed, A.M.A.; Elsaid, A.; Nour, H.M.; Elsonbaty, A. Dynamical behavior, chaos control and synchronization of a memristor-based ADVP circuit. *Commun. Nonlinear Sci. Numer. Simul.* **2013**, *18*, 148–170.
37. Mahmoud, G.M.; Bountis, T.; AbdEl-Latif, G.M.; Mahmoud, E.E. Chaos synchronization of two different chaotic complex Chen and Lü systems. *Nonlinear Dyn.* **2009**, *55*, 43–53.
38. Zhou, P.; Bai, R.; Zheng, J. Projective synchronization for a class of fractional-order chaotic systems with fractional-order in the (1, 2) interval. *Entropy* **2015**, *17*, 1123–1134.
39. Huang, J.; Li, C.; Huang, T.; Wang, H.; Wang, X. Synchronization and lag synchronization of hyperchaotic memristor-based Chua's circuits. *Math. Probl. Eng.* **2014**, *2014*, doi:10.1155/2014/203123.
40. Jin-E, Z. Combination-combination hyperchaos synchronization of complex memristor oscillator system. *Math. Probl. Eng.* **2014**, *2014*, doi:10.1155/2014/591089.
41. Zhou, X.; Jiang, M.; Huang, Y. Combination synchronization of three identical or different nonlinear complex hyperchaotic systems. *Entropy* **2013**, *15*, 3746–3761.
42. Chua, L.O. Memristor-The missing circuit element. *IEEE Trans. Circuit Theory* **1971**, *18*, 507–519.

© 2015 by the authors; licensee MDPI, Basel, Switzerland. This article is an open access article distributed under the terms and conditions of the Creative Commons Attribution license (http://creativecommons.org/licenses/by/4.0/).